NIH Public Access
Author Manuscript
J Phys Chem Lett. Author manuscript; available in PMC 2011 July 1.

Published in final edited form as:
J Phys Chem Lett. 2010 July 1; 1(13): 1973–1976. doi:10.1021/jz100683t.

Diffusion-Influenced Transport of Ions across a Transmembrane Channel with an Internal Binding Site

Huan-Xiang Zhou*
Department of Physics and Institute of Molecular Biophysics, Florida State University, Tallahassee, FL 32306, USA

Abstract

We develop a microscopic theory for ion transport across a transmembrane channel with an internal binding site. The ion flux is determined by the rate constants for binding to the internal site from the two sides of the membrane and the corresponding unbinding rate constants. The binding rate constants are formulated in terms of diffusion-influenced reactions. The theory allows a reconciliation of experimental data on the conductance of the influenza A M2 proton channel with the structure and dynamics of the protein.

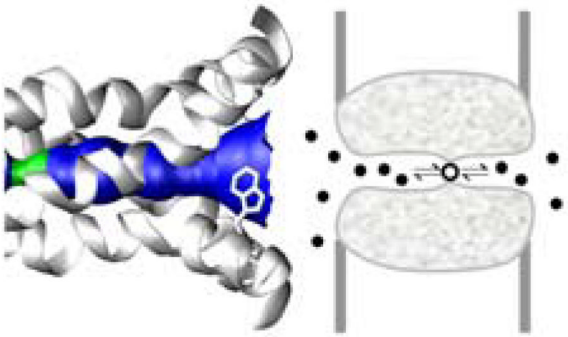

Keywords

Ion channels; ion transport; M2 proton channel; diffusion

In some transmembrane ion channels, the ion selected for transport obligatorily binds to an internal site, such as a protonation site like a histidine residue in a proton channel[1–4] or a site separated by energy barriers from the two opposite entrances of the channel.[5,6] One may model by chemical kinetics the binding and unbinding on either side of the internal site (Figure 1). Specifically, an ion on the left, signified with index 1, can take up the binding site, with rate constant k_{1+}, and an ion on the right side, signified with index 2, can take up the binding site, with rate constant k_{2+}. Once bound (from either side), the ion can unbind either to side 1, with rate constant k_{1-}, or to side 2, with rate constant k_{2-}. If the ion concentrations in the bulk solutions on the two sides of the membrane are C_i, the steady-state ion flux per channel is[5]

*Correspondence information: phone, (850) 645-1336; fax, (850) 644-7244; hzhou4@fsu.edu.

NIH-PA Author Manuscript
NIH-PA Author Manuscript
NIH-PA Author Manuscript

NIH-PA Author Manuscript

NIH-PA Author Manuscript

NIH-PA Author Manuscript

$$I=\frac{(k_{1+}k_{2-}C_1 - k_{2+}k_{1-}C_2)/(k_{1-}+k_{2-})}{1+\frac{k_{1+}C_1+k_{2+}C_2}{k_{1-}+k_{2-}}}. \quad (1)$$

The aim of this Letter is to present a theory for calculating the rate constants from a microscopic formulation of the binding process and use the resulting theory to characterize the structure-dynamics-function correlation of the influenza A M2 proton channel. The proton conductance function of the M2 protein is essential for viral replication.

In the M2 proton channel, the obligatory binding site is provided by the His 37 tetrad (Figure 1c).[7,8] In bulk solution, the rate constant of proton binding to a histidine sidechain, i.e., an imidazole, is 10^{10} $M^{-1}s^{-1}$.[9] Such a high binding rate constant suggests diffusion control. Diffusion-controlled proton binding to imidazole can be modeled as absorption of diffusing protons by a patch on an otherwise reflecting spherical surface. When the patch spans 60° in polar angle, the rate constant is ~$2\pi Da_0$,[10] where D is the proton diffusion constant and a_0 is the proton-imidazole contact radius. The observed rate constant is reproduced with the measured proton diffusion constant[11] of 10^3 $Å^2$/ns and a_0 = 2.6 Å, a size that seems quite reasonable. A binding site in the channel pore is much less accessible than its counterpart in bulk solution, and hence the diffusion-limited binding rate constant would be reduced.[12,13] Consequently there is all the more reason to model proton binding to the His37 tetrad in the pore of the M2 protein as diffusion-controlled.

The binding rate constants k_{i+} and the corresponding unbinding rate constants k_{i-} are related by the dissociation constants:

$$\frac{k_{i-}}{k_{i+}}=K_{\mathrm{d}i}, i=1 \text{ and } 2. \quad (2)$$

The two dissociation constants $K_{\mathrm{d}1}$ and $K_{\mathrm{d}2}$ are related, since they describe the binding equilibra of the same species, i.e., the permeating ion to the same site. When the excess chemical potentials of the ion in the bulk solutions on the two sides of the membrane are the same, then we must have $K_{\mathrm{d}1} = K_{\mathrm{d}2}$; hereafter we refer to this value as the intrinsic dissociation constant and denote it as K_{d}^0. Note that, in this case, as expected, the ion flux given by eq (1) is zero when $C_1 = C_2$. More generally, when there is a difference, say ΔU, in excess chemical potential on going from the bulk solution on side 1 to the bulk solution on side 2, e.g., due to a voltage across the membrane, then corresponding differences, ΔU_1 and ΔU_2, respectively, exist between the binding site and the bulk solutions on the two sides; $\Delta U_1 - \Delta U_2, = \Delta U$. Consequently

$$K_{\mathrm{d}i}=K_{\mathrm{d}}^0 e^{\Delta U_i/k_{\mathrm{B}}T}, \quad (3a)$$

$$\frac{K_{\mathrm{d}2}}{K_{\mathrm{d}1}}=e^{-\Delta U/k_{\mathrm{B}}T}, \quad (3b)$$

where k_{B} is the Boltzmann constant and T the absolute temperature. Hereafter $(k_{\mathrm{B}}T)^{-1}$ will be denoted as β. We take K_{d}^0 as given; that allows us to focus on the binding rate constants k_{i+}.

NIH-PA Author Manuscript

NIH-PA Author Manuscript

NIH-PA Author Manuscript

In our model, k_{i+} are diffusion-influenced rate constants for binding to a "buried" site. For notational simplicity, we specialize our description to the binding from one side, say side 1, and drop the index i for now. By applying the so-called constant-flux approximation[10] on the channel entrance, k_+ can be calculated by solving two simpler problems.[12] The first is the "exterior" problem, for the diffusion-controlled binding of ions from the bulk solution to the channel entrance. For a circular entrance with radius a, the binding rate constant for the exterior problem is $k_{ex} = 4Da$.[14]

The second is the "interior" problem, for the diffusion-influenced binding of ions in the pore to the internal site, with a special boundary condition at the channel entrance. We model the motion of ions in the pore (between the channel entrance and the binding site) as one-dimensional diffusion along the channel axis, with the coordinate denoted as x. The diffusion may be influenced by a potential energy function, $U(x)$, arising from interactions with the pore or an external voltage. The cross section, $\sigma(x)$, along the pore may be non-uniform; then $\sigma(x)$ effectively contributes an entropic term to the energy function.[15] The channel entrance and the binding site are assumed to be located at $x = 0$ and $x = d$, respectively. The rate constant, k_{in}, for the interior problem is given by the flux of the steady-state diffusion equation, when the binding site is modeled as an absorbing boundary condition (or a radiation boundary condition when binding is only partially controlled by diffusion). For a cylindrical pore with radius a and a linear potential $U(x) = \alpha x$, we find

$$k_{in}=\pi D a^2 \alpha\beta/(e^{\alpha\beta d} - 1). \quad (4)$$

When the pore is cone-shaped (see Figure 1b and 1c), with radius a at the binding site, radius a_2 at the pore entrance, and length d_2 along the pore axis, and the potential is zero, we have

$$k_{in}=\pi D a a_2/d_2. \quad (5)$$

The overall binding rate constant is[12]

$$\frac{1}{k_+}=\frac{1}{k_{ex}}+\frac{1}{k_{in}}. \quad (6)$$

In Figure 2a, we show the flux for a cylindrical proton channel with a binding site located at d = 21 Å, or 60% through the full pore length of 35 Å, when the pH on one side is fixed at 7 while the pH on the other side is varied from 7 to 3. With $D = 10^3$ Å^2/ns and a pore radius of a = 3 Å, the rate constants for proton binding from the two sides are 0.7×10^9 and 10^9 $M^{-1}s^{-1}$, respectively. That $k_{2+} > k_{1+}$ here is because the binding site is closer to the channel entrance on side 2 than to its counterpart on side 1. The intrinsic dissociation constant of the internal binding is set to 10^{-6} M, corresponding to the third pK_a of ~6 for the His37 tetrad of the M2 protein.[7,8] The proton flux in either direction shows saturation as the varying pH is below 4, but the saturation values in the two directions are different. According to eq (1), the saturation value of the flux is k_{2-} for the 1→2 flux (when protons are driven from side 1 to side 2) and k_{1-} for the 2→1 flux. These unbinding rate constants are given by $K_d^0 k_{i+}$. The asymmetry between the fluxes in the two directions is thus due to the asymmetry in k_{i+}. The asymmetric and saturable fluxes shown here are qualitatively consistent with conductance measurements on the M2 protein.[16] For the parameters listed above, the saturation value of the 1→2 flux is 1000 ions per channel per second. In Figure 2b, we show the flux-voltage relation for three pH gradients: $pH_1 = 6$, $pH_2 = 8$; $pH_1 = 8$, $pH_2 = 6$; and $pH_1 = pH_2 = 6$. Again, these

NIH-PA Author Manuscript

NIH-PA Author Manuscript

NIH-PA Author Manuscript

results are qualitatively consistent with voltage dependences of proton currents conducted by the M2 protein.[2,16]

However, the results of Figure 2 overestimate the magnitudes of the observed proton fluxes, which are of the order of 100 protons per channel per second.[2,17,18] Our model for the channel assumes a static structure for the protein, in which the binding site is always accessible to protons from the bulk solutions on both sides. In contrast, molecular dynamics (MD) simulations show that the channel is closed on both sides most of the time, and conformational gating allows protons to occasionally access the binding site.[19] The ion binding rate constants are thus lower than calculated by assuming an always open channel,[12,13] leading to a reduced proton flux. We now examine the effects of conformational gating on proton flux.

It has long been known that Trp41 plays an important gating role in the M2 channel.[20] MD simulations further show that the gating motion of Trp41 is coupled to the global deformation of the transmembrane helix, in the form of kinking around Gly34.[4] As previously proposed,[4] there are two conformational states (see Figure 1c): the open state involves significant helix kinking, leading to a wider opening of the pore toward the C-terminal end (which hereafter is identified with side 2), whereas in the closed state the helix is relatively straight. Equation (1) for the ion flux can be generalized to the case where the channel protein interconverts between two conformational states.[5] Under the condition that the conformational interconversion is much faster than proton binding/unbinding, eq (1) still holds but the rate constants are weighted averages of the two conformations. We argue that this condition is fulfilled by the M2 protein.[21] Since only the open conformation is competent in proton binding from the C-terminal side, conformational averaging leads to

$$k_{2+}^{\mathrm{avg}} = p_{\mathrm{open}} k_{2+}, \tag{7}$$

where p_{open} is the probability of the M2 protein being in the open conformation and k_{2+} is the diffusion-controlled rate constant for proton binding from the C-terminal side in that conformation.

For a cone-shaped pore with a = 3 Å, a_2 = 5 Å, and d_2 = 14 Å, k_{2+} is calculated to be 2×10^9 $M^{-1}s^{-1}$. A k_{2+}^{avg} value that is 10-fold lower than the k_{2+} value in Figure 2 is achieved if it is assumed that the M2 protein has only a 5% probability of being in the open conformation. That the open conformation is a minor population is consistent with MD simulations[4] and the observation that NMR peaks remain in essentially the same positions upon lowering pH.[22]

On the N-terminal side, Yi et al.,[19] based on MD simulations, proposed that Val27 near the channel entrance serves as a “secondary” gate (see Figure 1c). The effect of a gate that stochastically switches between open and closed on the binding rate constant has been studied previously.[12] The stochastically gated rate constant, k_{1+}^{sg}, like the counterpart k_{1+} for an always open channel, is calculated by separately solving the exterior and interior problems. The result for diffusion-controlled binding in a cylindrical channel without a potential is

$$\frac{1}{k_{1+}^{\mathrm{sg}}} = \frac{1}{k_{1+}} + \frac{\omega_c}{\omega_o}\left[\frac{1}{\omega \hat{k}_{\mathrm{ex}}(\omega)} + \frac{\tanh(\omega d^2/D)^{1/2}}{\pi a^2 (D\omega)^{1/2}}\right], \tag{8}$$

where ω_c and ω_o are the open-closed transition rates of the gate, located at the channel entrance; $\omega = \omega_c + \omega_o$; and $\hat{k}_{\mathrm{ex}}(s)$ is the Laplace transform of the time-dependent rate coefficient for the exterior problem. For a circular channel entrance, a very accurate result is[23]

NIH-PA Author Manuscript

NIH-PA Author Manuscript

NIH-PA Author Manuscript

$$s\widehat{k}_{ex}(s)/4Da=1+(\pi/4)(sa^2/D)^{1/2}-\frac{(1-\pi/4)(sa^2/D)^{1/2}}{(1-\pi/4)\pi/2(\pi^2/8-1)+(sa^2/D)^{1/2}}. \quad (9)$$

When $\omega \ll D/d^2$ and D/a^2, eq (8) reduces to

$$k_{1+}^{sg}=(\omega_o/\omega)k_{1+}. \quad (10)$$

At $\omega_o = 0.1\ ns^{-1}$ and $\omega_c = 1\ ns^{-1}$ (along with the other parameters used in Figure 2), k_{1+}^{sg} is close to the limit of eq (10), and is reduced from k_{1+} by 10-fold. These illustrative transition rates have timescales and relative magnitudes that are consistent with the dynamics of the Val27 secondary gate seen in simulations.[19] Note that the conformational interconversion important for proton binding from the C-terminal side has little effect on the binding rate constant from the N-terminal side, since the two conformations do not differ significantly in the N-terminal half (Figure 1c).

The 10-fold reductions in k_{i+} by conformational gating bring the magnitude of the calculated proton flux into agreement with experimental values. Several mutations that presumably affect gating dynamics provide further test of our analysis of its effects on proton flux. For example, a mutation of Gly34 into alanine is expected to rigidify the helix backbone and hence reduce the probability of the open conformation, which we propose to be required for proton binding from the C-terminal side. Consistent with this expectation, the G34A mutation reduces the conductance of the M2 protein by 60%.[24] On the other hand, mutating the secondary gate residue Val27 into a smaller alanine is expected to increase the open gate probability on the N-terminal side and hence increase proton flux. Indeed, the V27A mutation leads to a 50% increase in conductance.[24]

In summary, we have presented a microscopic theory for ion transport across a channel with an internal binding site. With this theory, we have rationalized the observed low, asymmetric, and saturable conductance of the influenza M2 proton channel in terms of the structural and dynamical properties of the protein.

Acknowledgments

This work was supported in part by Grants GM58187 and AI23007 from the National Institutes of Health. I thank David Busath for reading the manuscript.

References and Notes

1. Pinto LH, Dieckmann GR, Gandhi CS, Papworth CG, Braman J, Shaughnessy MA, Lear JD, Lamb RA, DeGrado WF. A Functionally Defined Model for the M2 Proton Channel of Influenza a Virus Suggests a Mechanism for Its Ion Selectivity. Proc. Natl. Acad. Sci. USA 1997;94:11301–11306. [PubMed: 9326604]
2. Mould JA, Li HC, Dudlak CS, Lear JD, Pekosz A, Lamb RA, Pinto LH. Mechanism for Proton Conduction of the M_2 Ion Channel of Influenza a Virus. J. Biol. Chem 2000;275:8592–8599. [PubMed: 10722698]
3. Khurana E, Peraro MD, Devane R, Vemparala S, Degrado WF, Klein ML. Molecular Dynamics Calculations Suggest a Conduction Mechanism for the M2 Proton Channel from Influenza a Virus. Proc. Natl. Acad. Sci. USA 2009;106:1069–1074. [PubMed: 19144924]

NIH-PA Author Manuscript NIH-PA Author Manuscript NIH-PA Author Manuscript

4. Yi M, Cross TA, Zhou HX. Conformational Heterogeneity of the M2 Proton Channel and a Structural Model for Channel Activation. Proc. Natl. Acad. Sci. USA 2009;106:13311–13316. [PubMed: 19633188]
5. Lauger P, Stephan W, Frehland E. Fluctuations of Barrier Structure in Ionic Channels. Biochim. Biophys. Acta 1980;602:167–180. [PubMed: 6251885]
6. Lauger P. Ionic Channels with Conformational Substates. Biophys. J 1985;47:581–590. [PubMed: 2410042]
7. Hu J, Fu R, Nishimura K, Zhang L, Zhou HX, Busath DD, Vijayvergiya V, Cross TA. Histidines, Heart of the Hydrogen Ion Channel from Influenza a Virus: Toward an Understanding of Conductance and Proton Selectivity. Proc. Natl. Acad. Sci. USA 2006;103:6865–6870. [PubMed: 16632600]
8. The M2 protein functions as a tetramer; hence the His37 tetrad provides four protonation sites. The channel becomes activated when viral exterior pH is lowed to ~6. At this pH, two protons are always bound to the His37 tetrad (ref 7); it is the binding of the third proton that leads to channel conductance. Hence what we model here is the binding/unbinding of a proton to/from a doubly protonated His37 tetrad. That the doubly protonated His37 tetrad has two equivalent protonation sites serves to double the binding and unbinding rate constants. Here we model the two protonation sites together as an absorbing disk.
9. Eigen M, Hammes GG. Elementary Steps in Enzyme Reactions (as Studied by Relaxation Spectrometry). Adv. Enzymol. Relat. Areas Mol. Biol 1963;25:1–38. [PubMed: 14149678]
10. Shoup D, Lipari G, Szabo A. Diffusion-Controlled Bimolecular Reaction Rates. The Effect of Rotational Diffusion and Orientation Constraints. Biophys. J 1981;36:697–714. [PubMed: 7326330]
11. Roberts NK, Northey HL. Proton and Deuteron Mobility in Normal and Heavy Water Solutions of Electrolytes. J. Chem. Soc., Faraday Transactions I 1974;70:253–262.
12. Zhou H-X. Theory of the Diffusion-Influenced Substrate Binding Rate to a Buried and Gated Active Site. J. Chem. Phys 1998;108:8146–8154.
13. Zhou H-X, Wlodek ST, McCammon JA. Conformation Gating as a Mechanism for Enzyme Specificity. Proc. Natl. Acad. Sci. USA 1998;95:9280–9283. [PubMed: 9689071]
14. Hill TL. Effect of Rotation on Diffusion-Controlled Rate of Ligand-Protein Association. Proc. Natl. Acad. Sci. USA 1975;72:4918–4922. [PubMed: 1061081]
15. Zhou H-X, Zwanzig R. A Rate Process with an Entropy Barrier. J. Chem. Phys 1991;94:6147–6152.
16. Chizhmakov IV, Ogden DC, Geraghty FM, Hayhurst A, Skinner A, Betakova T, Hay AJ. Differences in Conductance of M2 Proton Channels of Two Influenza Viruses at Low and High Ph. J. Physiol 2003;546:427–438. [PubMed: 12527729]
17. Lin TI, Schroeder C. Definitive Assignment of Proton Selectivity and Attoampere Unitary Current to the M2 Ion Channel Protein of Influenza a Virus. J. Virol 2001;75:3647–3656. [PubMed: 11264354]
18. Moffat JC, Vijayvergiya V, Gao PF, Cross TA, Woodbury DJ, Busath DD. Proton Transport through Influenza a Virus M2 Protein Reconstituted in Vesicles. Biophys. J 2008;94:434–445. [PubMed: 17827230]
19. Yi M, Cross TA, Zhou H-X. A Secondary Gate as a Mechanism for Inhibition of the M2 Proton Channel by Amantadine. J. Phys. Chem. B 2008;112:7977–7979. [PubMed: 18476738]
20. Tang Y, Zaitseva F, Lamb RA, Pinto LH. The Gate of the Influenza Virus M2 Proton Channel Is Formed by a Single Tryptophan Residue. J. Biol. Chem 2002;277:39880–39886. [PubMed: 12183461]
21. The conformational interconversion occurs on timescales much shorter than 1 ms, as indicated by the observation that NMR spectra remain to have single, albeit broadened, peaks upon lowering pH to a range where the channel becomes conducting (ref 22), whereas proton binding/unbinding, as indicated by the (effective) rate constants k_i+C_i and k_{i-}, occurs on the ms timescale.
22. Li C, Qin H, Gao FP, Cross TA. Solid-State NMR Characterization of Conformational Plasticity within the Transmembrane Domain of the Influenza a M2 Proton Channel. Biochim. Biophys. Acta 2007;1768:3162–3170. [PubMed: 17936720]
23. Zwanzig R, Szabo A. Time Dependent Rate of Diffusion-Influenced Ligand Binding to Receptors on Cell Surfaces. Biophys. J 1991;60:671–678. [PubMed: 1657231]

NIH-PA Author Manuscript

NIH-PA Author Manuscript

NIH-PA Author Manuscript

24. Balannik V, Carnevale V, Fiorin G, Levine BG, Lamb RA, Klein ML, DeGrado WF, Pinto LH. Functional Studies and Modeling of Pore-Lining Residue Mutants of the Influenza a Virus M2 Ion Channel. Biochemistry 2010;49:696–708. [PubMed: 20028125]

NIH-PA Author Manuscript

NIH-PA Author Manuscript

NIH-PA Author Manuscript

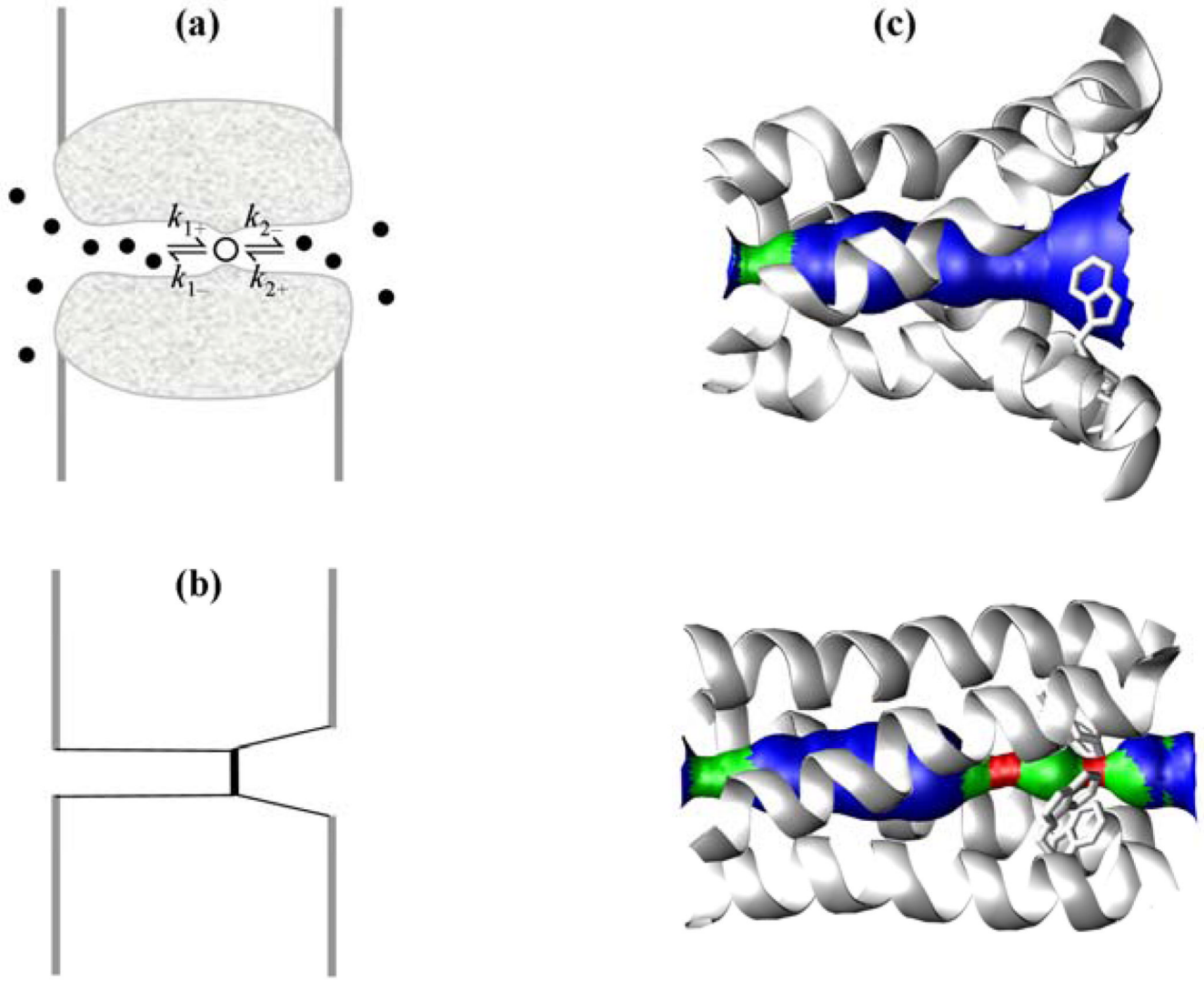

Figure 1.

A transmembrane ion channel with an internal binding site. (a) Diffusion of ions into the pore and binding at the internal site. (b) Idealized geometry of the pore. (c) Open and closed conformations of the M2 proton channel, which consists of four identical helical subunits. Top: open conformation in which proton binding from the C-terminal side (on the right) is allowed. Bottom: closed conformation in which proton binding from the C-terminal side is prohibited by the primary gate residue Trp41, which is shown as sticks. The constriction on the left comes from Val27; the constriction near the middle of the pore seen in the bottom panel comes from His37, which is the proton binding site. Part (c) is adapted from Yi et al.[4] with permission; copyright (2009) the National Academy of Sciences, U.S.A.

NIH-PA Author Manuscript

NIH-PA Author Manuscript

NIH-PA Author Manuscript

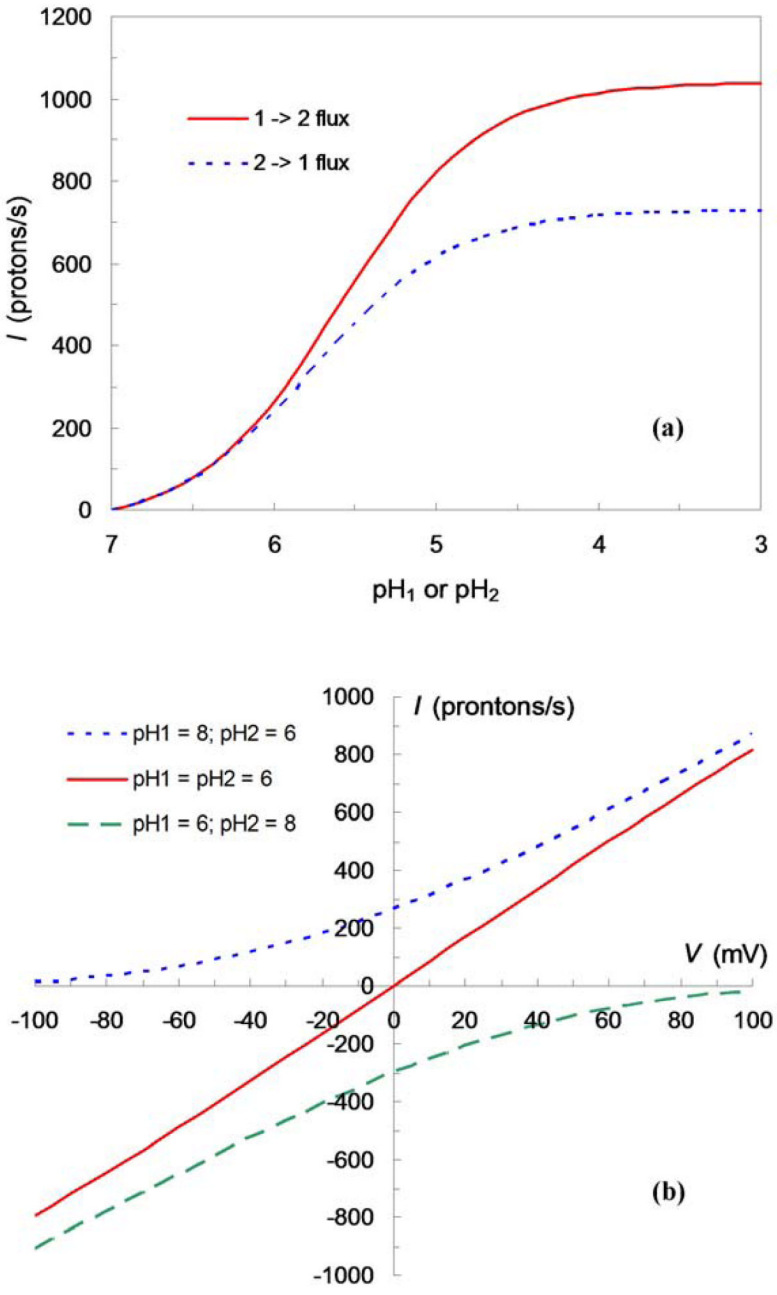

Figure 2.

Ion fluxes driven by (a) pH gradient and (b) voltage. A cylindrical pore, with radius $a = 3$ Å and full length $L = 35$ Å, is assumed; binding to the internal site, located at $d = 15$ Å, is diffusion-controlled. The proton diffusion constant D is 10^3 Å^2/ns. When a voltage V is applied across the membrane, the potential function in the pore is taken to be a linear function: $U(x) = eVx/L$, where e is the proton charge.